

Theoretical and Experimental Characterization of Nonsymmetrically Shielded Coplanar Waveguides for Millimeter-Wave Circuits

FERDINANDO ALESSANDRI, UHLAND GOEBEL, FRANCO MELAI, MEMBER, IEEE, AND ROBERTO SORRENTINO, SENIOR MEMBER, IEEE

Abstract — A new quasi-planar structure, the nonsymmetrically shielded coplanar waveguide (NSCPW), is proposed as a quasi-TEM transmission line with advantageous characteristics for millimeter-wave circuit applications. Advantages in terms of broad-band behavior and ease of machining, as well as device mounting and substrate mounting, are pointed out. An experimental method has been developed which allows the evaluation of the transmission line spectrum in a very wide frequency band (15:1) with a single transmission measurement. The propagation characteristics of the dominant and higher order modes evaluated experimentally are shown to be in excellent agreement with the theoretical predictions based on the generalized transverse resonance technique. This method has also been used for an extensive characterization of the structure in terms of characteristic impedance and useful frequency band.

I. INTRODUCTION

A NUMBER OF different transmission lines have been proposed for applications in the millimeter-wave range [1]. *E*-plane and suspended line structures seem to be the most viable candidates for applications in the range from 60 to 100 GHz. These transmission lines belong to the class of quasi-planar circuits. They combine the advantages of waveguides in terms of low loss and planar circuits in terms of integration capabilities.

Despite their advantages with respect to passive millimeter-wave circuits, the above-mentioned technologies exhibit some difficulties with respect to active device embedding, e.g. for amplifiers or oscillators. For instance, the finite cutoff frequency of finlines implies reactive loading of active devices at low frequencies, which may cause stability problems. Also the intrinsic isolation between adjacent circuit elements is poor, resulting in unwanted feedback paths. Suspended line, on the other hand, makes device mounting difficult, often resulting in increased parasitics and degraded performances of both packaged and unpackaged devices.

In this paper we propose a modified structure combining the advantages of both finline and suspended stripline. It consists of a coplanar waveguide inserted into a non-

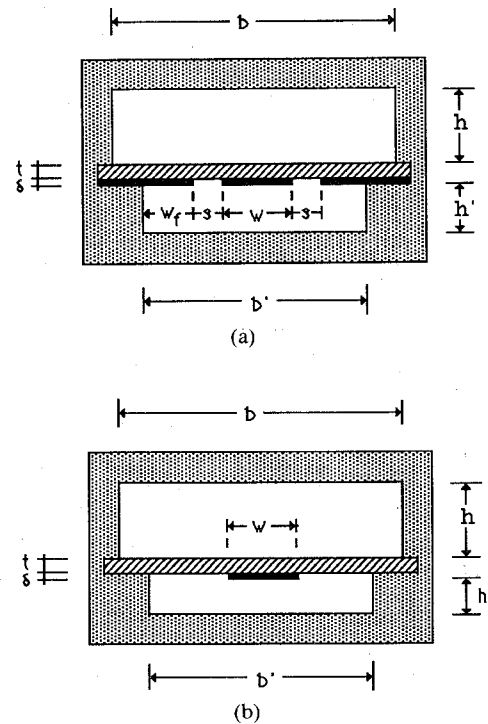


Fig. 1. Cross-sectional geometries of (a) the NSCPW and (b) the NSSS.

symmetrical housing. The cross-sectional geometry of the nonsymmetrically shielded coplanar waveguide (NSCPW) is shown in Fig. 1(a). By simply eliminating the grounded metal fins we obtain the nonsymmetrical suspended substrate stripline (NSSS), Fig. 1(b). The unsymmetrical construction of the split-block housing simplifies circuit mounting by soldering or epoxy-bonding it to one half housing. Critical mechanical tolerances and contacts at mounting grooves can be circumvented in this way.

The quasi-TEM propagation of both variants allows broad-band matched device embedding, which makes the present structure substantially different from the unsymmetrical finline proposed in [2]. A wide range of characteristic impedances and different field configurations can be achieved by changing between NSCPW and NSSS. The former is well matched to packaged transistors, since most

Manuscript received April 4, 1989; revised July 19, 1989.

F. Alessandri and R. Sorrentino are with the University of Rome "Tor Vergata," Via Raimondo, Rome, Italy 00173.

U. Goebel and F. Melai are with the Millimeter-Wave Department, Micrel S.p.A., Florence, Italy.

IEEE Log Number 8930954.

of the electric field is concentrated in the plane of the substrate involving less field distortion in the vicinity of the transistor housing. NSSS has pronounced low-loss performance, since most of the field is concentrated in the air gap between the strip and the housing wall.

NSCPW is best suited for:

- mounting of beam lead and three-terminal solid-state devices;
- matching elements in both series and shunt configurations;
- biasing circuits.

NSSS on the other hand, is useful for:

- filters (e.g. end coupled bandpass, broadside-coupled bandstop filters);
- directional couplers and power splitters;
- low-loss line sections and transitions to waveguides.

Both theoretical and experimental investigations of the NSCPW/NSSS structures have been carried out and are presented in this paper.

A sophisticated analysis method is required to solve the associated boundary value problem, including the effect of the metallization thickness and optional mounting grooves. One such technique is the transverse resonance method, which is adopted here and is briefly reviewed in Section II. A simple, yet very accurate, experimental method has also been developed which allows a broad-band evaluation of the modal spectrum of the structures. This is described in Section III. An excellent agreement between theory and experiments has been obtained, as demonstrated by the results presented in Section IV. Based on theoretical computations, design curves in terms of characteristic impedance and usable frequency range are also given for a number of different configurations.

II. METHOD OF ANALYSIS

The method of analysis is the generalized transverse resonance method, which has been described in a number of papers [3]–[7]. The symmetry of the cross section can be used to analyze only one half of the structure, upon replacement of the symmetry plane with a magnetic wall (or an electric wall for odd-symmetric modes). The reduced cross section is shown in Fig. 2(a). (The metallization thickness has been exaggerated for illustration purposes.) Furthermore, we insert two electric walls at distance L one from the other so as to form a resonant cavity. In this manner, the longitudinal z dependence is in the form of a standing wave with spatial frequency

$$\beta = n\pi/L \quad (1)$$

n being the number of half wavelengths contained in the length L .

As seen in the x direction normal to the substrate, the structure appears as the connection of four rectangular waveguides (see Fig. 2(a)) with the same width L but different heights.

Fig. 2(b) shows the corresponding generalized equivalent transverse circuit. Each waveguide section is represented

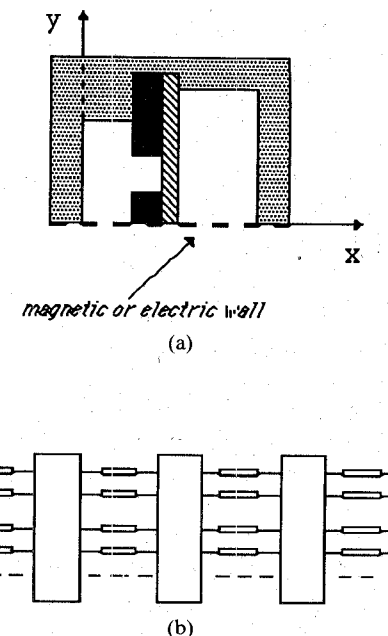


Fig. 2. (a) Reduced cross section of NSCPW for analysis and (b) generalized equivalent transverse circuit.

by a theoretically infinite number of transmission lines, each corresponding to a different mode. In actual computations only finite numbers of modes can be used. Contrary to [5] and [6], however, in the present formulation a different number of modes, proportional to the height, is chosen in each section in order to properly account for the relative convergence phenomenon [8], [9]. In this manner the computational effort is minimized. The field equations, in fact, can be manipulated so as to reduce all the unknowns to those of the narrower section, thus obtaining a system of small size. For the same accuracy, a considerably higher number of modes would be required by choosing the same number of modes in each section as in [5] and [6].

The step discontinuities between the waveguide sections produce the coupling among the waveguide modes [10] and are represented by generalized multiport networks.

Using the formalism of the *Waveguide Handbook* [11], the transverse-to- x components of the EM field can be written in the i th waveguide section as

$$\mathbf{E}_t^{(i)} = \sum_m V_m^{(i)}(x) \mathbf{e}_m^{(i)}(y, z) \quad (2)$$

$$\mathbf{H}_t^{(i)} = \sum_m I_m^{(i)}(x) \mathbf{h}_m^{(i)}(y, z) \quad (3)$$

where the $\mathbf{e}_m^{(i)}$'s and $\mathbf{h}_m^{(i)}$'s are obtained from the scalar potentials relative to $\text{TE}^{(x)}$ and $\text{TM}^{(x)}$ modes. Their expressions are well known and are not given here.

The eigenvectors satisfy the orthonormal condition on the section S_i :

$$\int_{S_i} \mathbf{e}_m^{(i)} \cdot \mathbf{e}_n^{(i)} dS = \int_{S_i} \mathbf{h}_m^{(i)} \cdot \mathbf{h}_n^{(i)} dS = \delta_{mn} \quad (4)$$

where δ_{mn} is the Kronecker delta.

The V and I expansion coefficients in (2) and (3) correspond to voltages and currents on the equivalent transmission lines. The boundary conditions at each step

discontinuity relate voltages and currents at both sides. Using the orthonormality relations (4) one obtains [7]

$$V_n^{(i+1)} = \sum_m g_{nm} V_m^{(i)} \quad I_m^{(i)} = \sum_n g_{mn} I_n^{(i+1)} \quad (5)$$

where g_{mn} is the coupling coefficient between the m th mode of the i th guide and the n th mode of the $(i+1)$ th guide. In matrix form,

$$[V^{(i+1)}] = [G][V^{(i)}] \quad [I^{(i)}] = [G]^T [I^{(i+1)}]. \quad (6)$$

Equations (5) and (6) define the generalized multiports of Fig. 2(b).

The resonant condition of the generalized transverse equivalent circuit of Fig. 2(b) constitutes the dispersion relation for the structure, which has the form

$$f(\omega, \beta) = 0. \quad (7)$$

For any given distance L and resonant order n , (1) and (7) determine the resonant frequency f_{in} of the cavity for the i th mode and thus the frequency associated with the value of β given by (1). The complete spectrum of the transmission line can be determined by numerically simulating different resonant experiments either with different cavity lengths L or, if L is chosen large enough, increasing the resonant order n . The latter option corresponds to the experimental procedure described in the next section.

III. EXPERIMENTAL CHARACTERIZATION

To validate the theoretical results an experimental method has been developed to determine the propagation constants of all lower order modes across a very large (15:1) bandwidth. They can be obtained from only two broad-band transmission measurements of a two-port resonator formed by the waveguide structure under test. The two measurements correspond to the even- and odd-symmetrical modes, respectively.

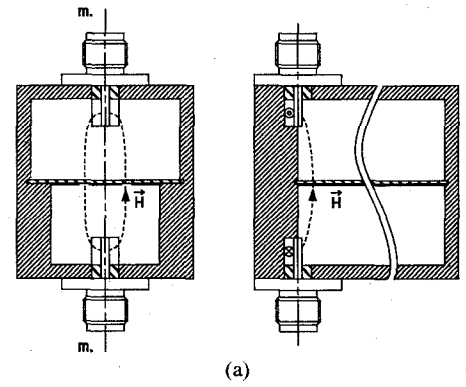
The following well-known methods:

- open end resonance line (with capacitive end-coupling),
- ring resonance technique,
- nodal shift technique,
- four short/four open technique,

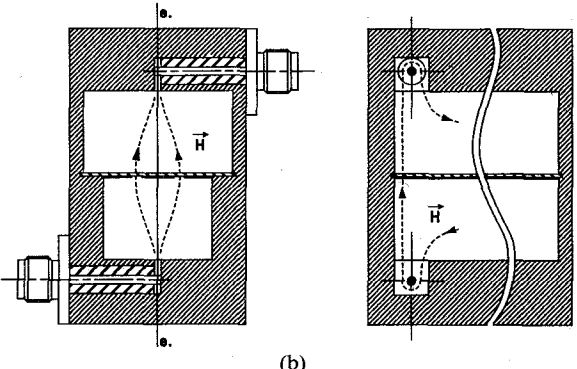
are only applicable to the fundamental mode and require at least two measurements on different line lengths to eliminate detuning effects introduced by the field coupling probes.

Instead, a method similar to [12] has been used where a small probe current was introduced into one of the two short circuits terminating a resonant microstrip line. For our measurements we used a completely closed cavity of about five wavelengths at center frequency with massive short-circuit plates at both ends.

A two-port resonator is realized by introducing one coaxial launcher above and another below the substrate at one end of the resonator. For even-mode excitation, the arrangement of Fig. 3(a) is used. By shorting the center conductors to ground and leaving part of the outer con-



(a)



(b)

Fig. 3. (a) Even-mode excitation arrangement showing magnetic field lines at dominant mode resonance (m.-m.: magnetic wall symmetry). (b) Odd-mode excitation arrangement showing magnetic field lines at resonance (e.-e.: electric wall symmetry).

ductor open to the waveguide, weak magnetic coupling with negligible detuning effect is obtained. Selective excitation of even-symmetrical modes is possible by orienting the coaxial launchers in the axial direction or perpendicular to the substrate, exciting transversal magnetic fields with magnetic wall symmetry ($m.-m.$).

Odd-symmetrical modes are excited with the center conductor oriented transversely to the longitudinal axis and parallel to the substrate. In this case the coaxial probes were not inserted directly into the waveguide. This was excited through small longitudinal slots milled in the center of the broad walls, as shown in Fig. 3(b).

With a proper choice of coupling aperture sizes, broad-band coupling is achieved to all modes of interest with small frequency variation. A local maximum of the transmission between the two coaxial ports occurs at every frequency where the cavity length is an integral multiple of $\lambda/2$ for one of the propagating modes excited. This is due to a maximum transverse magnetic field of the respective mode when a virtual short is transformed to the excited end of the resonator. Approximate magnetic field trajectories at resonance are shown in Fig. 3.

The contribution of the different modes to the resultant transmission can be explained by the approximate equivalent circuit of Fig. 4, which is an improved version of that in [13] and was found to fit the experiments very closely. The quantity n_i denotes the coupling coefficient (both mode- and frequency-dependent), Z_i is the multiple reso-

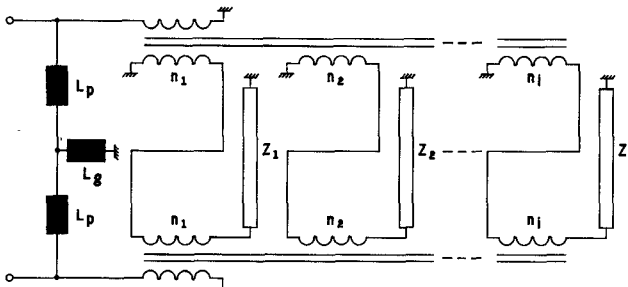


Fig. 4. Simplified equivalent circuit of the experimental setup.

nant input impedance of the i th mode, and L_p denotes the lumped shunt inductance of the shorted launchers. It has been verified experimentally by changing the center conductor length that even with strong coupling (a few dB of transmission loss) the detuning of resonant frequencies is less than 0.5 percent. L_p represents a common ground path, giving a small (-70 dB) basic coupling level at low frequencies. Due to the high Q (typically 500) of the individual resonances, their interference is very small. The mode number i and longitudinal order n can be determined directly from one broad-band swept frequency measurement. A typical measurement plot is shown in Fig. 5. Due to the absence of detuning effects, the propagation constant β_i of mode i at frequency f_{ni} can be determined using (1), or, in normalized form,

$$\frac{\beta_i}{k_0} = \frac{nc_0}{2Lf_{ni}}.$$

Typical transmission values are -30 to -5 dB, depending on the mode and the frequency.

IV. RESULTS

Two housings have been fabricated for experimental verifications, one for a NSCPW and one for a NSSS. With reference to Fig. 1, the dimensions are $b = 22.86$ mm, $b' = 15.8$ mm, and $h = b/2$ for both structures; $h' = h$ for the NSCPW; and $h' = 0.1b$ for the NSSS. The circuits were made on RT/duriod ($\epsilon_r = 2.2$) 0.254 mm thick. Metal thickness was 0.035 mm. The geometries of the metallizations were determined by the theory of Section II to have 100 and 50Ω characteristic impedances respectively: $w = 4.76$ mm and $s = 1.57$ mm for the NSCPW and $w = 10.00$ mm for the NSSS.

Transmission measurements were performed in the frequency range 0.5 to 15 GHz on cavities 15 cm long. This allowed the evaluation of the dispersion characteristics β versus f of the first three or two modes of the guiding structures. In the first experiments [13], the orientation of the coaxial probes was such that only the even-symmetrical characteristics were evaluated. To reutilize the circuits for further experiments it was decided not to solder the circuits to the housing. To properly hold the circuits and to ensure good electrical contact between the metal fins and the housing, grooves 0.5 mm deep were milled in the lower

housing. Grooves as well as the metal thickness were included in the theoretical simulations, although their effect is very small in the frequency range considered.

The theoretical and experimental results for the even-mode spectra of NSCPW and NSSS are compared in Fig. 6(a) and (b). Excellent agreement is observed. Error is always less than 2 percent and is generally around 1 percent. Both structures exhibit very low, practically negligible, dispersion of the dominant quasi-TEM mode. Because of its reduced housing height h' , in the frequency range examined the NSSS has only one propagating higher order mode instead of two as for the NSCPW.

Additional measurements were performed on structures obtained by interchanging the substrates with the housings. The theoretical and experimental results for these cases were again in very close agreement. It was found that the first two modes of both transmission lines were only slightly affected by the change in the height (h') of the lower half housing. The third mode, on the contrary, was seen to be shifted to much higher frequencies by reducing h' . This effect was more pronounced for the NSSS than for the NSCPW. This is due to the field concentration in the proximity of the metallization being higher in the NSCPW than in the NSSS.

An experimental investigation on the odd higher order modes was also performed, using identical waveguide housings except for the type of coupling, as described in the previous section. The agreement between experimental and theoretical predictions was again quite satisfactory, though slightly worse than for the even modes. An example of the results obtained is shown in Fig. 7 for the same NSCPW of Fig. 6(a).

It can be noted that a few experimental dots are missing in Figs. 6 and 7. In the higher frequency range, in fact, some of the resonances were not clearly detectable or could not be identified because of their high density or the excitation of spurious modes of the opposite symmetry.

A theoretical investigation has been carried out to characterize the transmission line in terms of bandwidth and characteristic impedance for various structural parameters. The characteristic impedance has been evaluated according to the voltage/power definition [4], i.e.,

$$Z_0 = |V|^2/(2P).$$

The characteristic impedances of the NSCPW and NSSS are shown in Fig. 8(a) and (b) as a function of the normalized strip width $w/(w+2s)$ for different values of the normalized height h'/b . All other parameters, including the fin separation ($w+2s$), are kept constant and are the same as for the experimental structures. Fig. 8 demonstrates a wide range of realizable characteristic impedances, from about 25 to over 200 Ω . It is observed also that in the case of the NSCPW, because of the field concentration in the proximity of the slots, the variation of Z_0 with h' is modest, except when h' is small.

The variation of Z_0 with $w/(w+2s)$ for different values of the normalized fin separation $(w+2s)/b'$ was also computed. The results were presented in [13] and are not

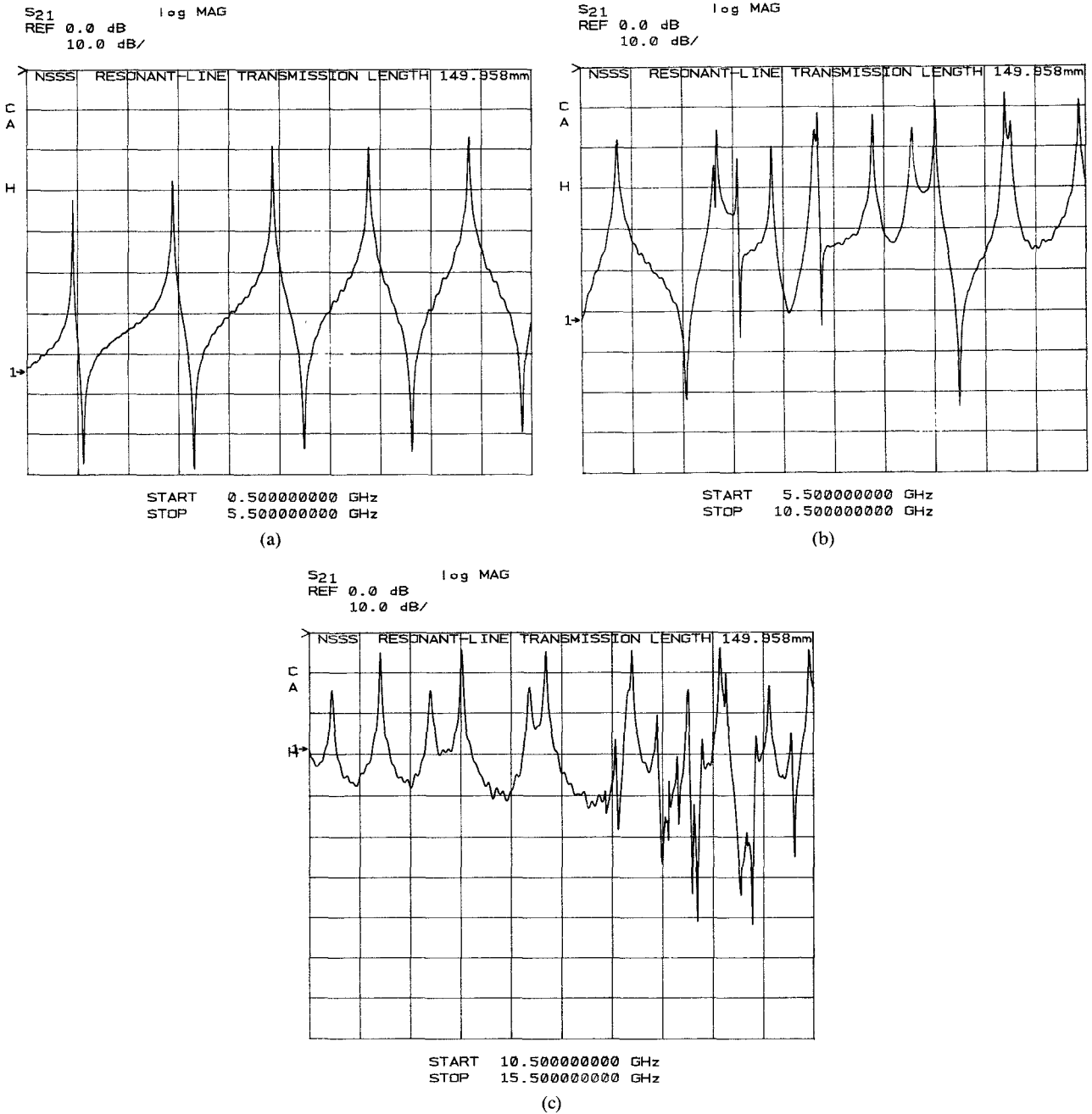


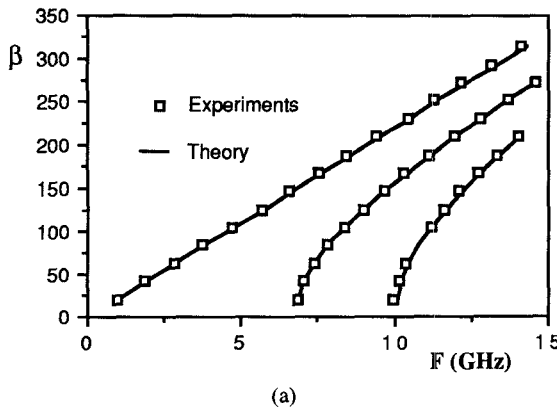
Fig. 5. Experimental transmission measurements of the NSSS structure in three frequency bands: (a) 0.5–5.5 GHz, (b) 5.5–10.5 GHz, (c) 10.5–15.5 GHz.

repeated here. In [13] the variations of the cutoff frequencies of the first higher modes as functions of $w/(w+2s)$ and h'/b were also shown. It was found that, contrary to the first odd mode, which is strongly affected by both strip width w and height h' of the lower half housing, the cutoff of the first higher mode with even symmetry is almost insensitive to both parameters and is practically coincident with that of the fundamental mode of the rectangular waveguide of width b .

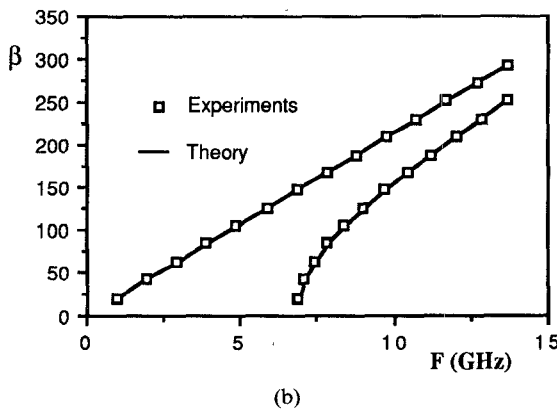
The characteristics of NSCPW's for use in the *Ka*-band have been investigated theoretically. Realistic values for the dimensions of the waveguide housing were chosen as follows: upper half waveguide $b = 2h = 3.22$ mm; lower housing $b' = 2.22$ mm; $h' = 0.25b = 0.805$ mm. A dielectric

substrate with $\epsilon_r = 3.75$ and a thickness of 0.154 mm with a metallization of 0.005 mm was assumed. The characteristic impedances for the NSCPW and NSSS cases are shown in Fig. 9 at the frequency of 35 GHz versus the shape ratio $w/(w+2s)$. Notice that, for a given shape ratio, the strip width of the NSSS is twice that of the NSCPW due to the fact that the fit separation is also doubled. For that reason the impedance curve of the NSSS lies below that of the NSCPW. By further reducing the strip width, the characteristic impedance of the NSSS can easily be increased over 200Ω (not shown in the figure).

Both NSCPW and NSSS configurations can be usefully employed in the same circuit due to their respective advantages. In the transition from one configuration to the other



(a)



(b)

Fig. 6. Theoretical and experimental even-mode spectra of (a) NSCPW and (b) NSSS.

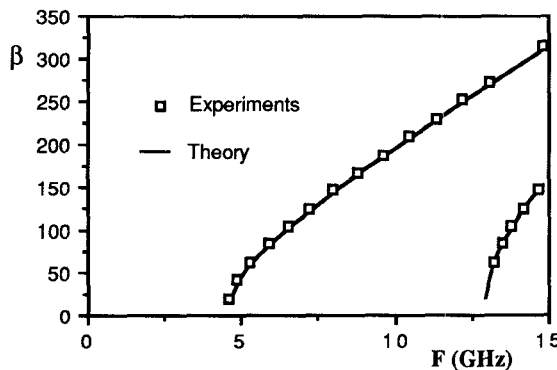


Fig. 7. Theoretical and experimental odd-mode spectra of the NSCPW of Fig. 6(a).

the same characteristic impedance must be maintained. Assuming the same strip width w for both configurations, the transition can be made by properly changing both the fin separation $w + 2s$ and the waveguide height h' in such a way that Z_0 is the same. Fig. 10 shows design curves for $Z_0 = 50$ and 100Ω . The normalized fin separation $(w + 2s)/b'$ width is plotted as a function of the aspect ratio h'/b' of the lower half housing. It can be observed that for the low impedance case ($Z_0 = 50 \Omega$), the slot width s is very small so that small variations of the fin separation must be compensated by relatively large variations of h' .

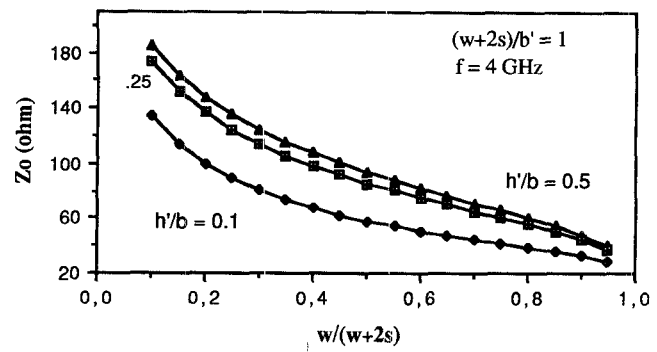
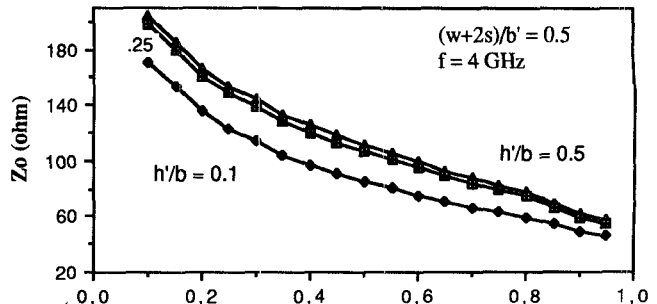


Fig. 8. Characteristic impedance of (a) the NSCPW and (b) the NSSS as a function of normalized strip width for different $((w + 2s)/b')$.

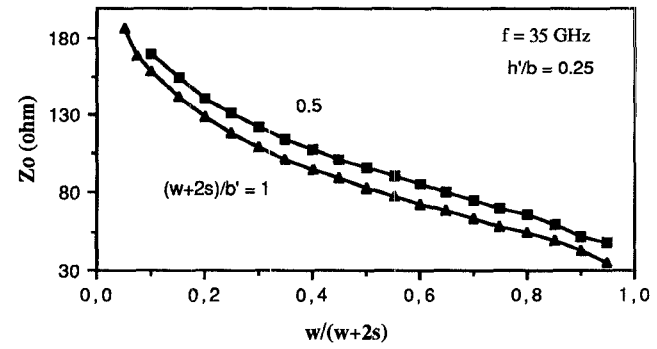


Fig. 9. Characteristic impedance of Ka-band NSCPW and NSSS as a function of normalized strip width.

The dispersive behavior of NSCPW and NSSS has finally been investigated. A comparison is made in Fig. 11 between structures with the same width and the same Z_0 (50 and 100Ω) as those corresponding to Fig. 10. No significant difference in terms of dispersion is observed. In all cases, an approximately linear increase of a few ohms in the whole band is observed.

V. CONCLUSIONS

A new quasi-planar structure, the nonsymmetrically shielded coplanar waveguide (NSCPW), has been proposed as a quasi-TEM transmission line with advantageous characteristics for millimeter-wave circuit applications. The elimination of the metal fins leads to a nonsymmetrically

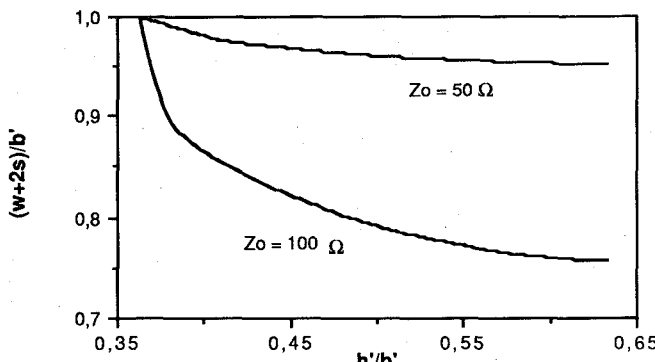


Fig. 10. Fin separation for constant 50 and 100 Ω characteristic impedances.

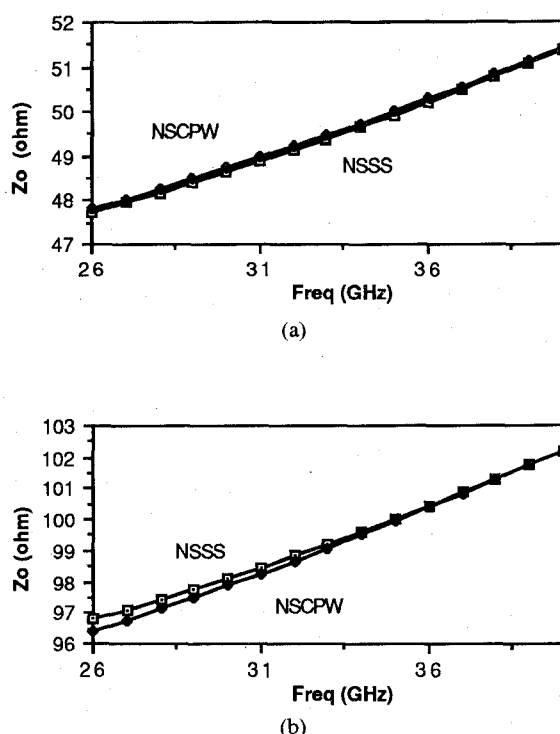


Fig. 11. Characteristic impedance frequency behavior of (a) 50 Ω and (b) 100 Ω NSCPW and NSSS. For both structures, $w = 1.86$ for (a) and 0.80 for (b). For the NSCPW, $s = 0.13$ mm for (a) and 0.46 mm for (b). For the NSSS, $h' = 0.8$. For the NSCPW, $h' = 1.2$ mm.

shielded suspended stripline (NSSS) which can be used in the realization of passive components due to its inherent low-loss properties. Advantages in terms of mechanical construction and circuit mounting have also been pointed out.

Experimental and theoretical investigations have been performed. An experimental technique has been developed which allows the complete evaluation of the line spectrum in a very wide frequency range with one transmission measurement for the dominant and even higher order modes and one transmission measurement for the odd higher order modes. Extremely good agreement has been demonstrated with the theoretical predictions based on the

generalized transverse resonance method. This method has also been used for an extensive characterization of the structure in terms of characteristic impedances and useful frequency bands.

ACKNOWLEDGMENT

The authors wish to thank S. Ghinassi of Micrel S.p.a. for his collaboration in the experimental activity.

REFERENCES

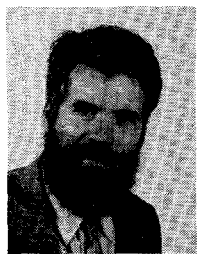
- [1] B. Bhat and S. K. Koul, *Analysis, Design and Applications of Fin Lines*, Norwood, MA: Artech House, 1987, ch. 1.
- [2] J. M. Goutoule, P. Espes, P. Fraise, and P. Combes, "Asymmetrical structure finline: An alternative for satellite applications," in *1986 IEEE MTT-S Int. Microwave Symp. Dig.* pp. 217-220.
- [3] R. Sorrentino and G. Leuzzi, "Full-wave analysis of integrated transmission lines on layered lossy media," *Electron. Lett.* vol. 18, no. 14, pp. 607-609, July 1982.
- [4] R. Sorrentino, G. Leuzzi, and A. Silbermann, "Characteristics of metal-insulator-semiconductor coplanar waveguides for monolithic microwave circuits," *IEEE Trans. Microwave Theory Tech.*, vol. MTT-32, pp. 410-416, Apr. 1984.
- [5] R. Vahldieck, "Accurate hybrid-mode analysis of various finline configurations including multilayered dielectrics, finite metallization thickness, and substrate holding grooves," *IEEE Trans. Microwave Theory Tech.*, vol. MTT-32, pp. 1454-1460, Nov. 1984.
- [6] R. Vahldieck and J. Bornemann, "A modified mode-matching technique and its application to a class of quasi-planar transmission lines," *IEEE Trans. Microwave Theory Tech.*, vol. MTT-33 pp. 916-926, Oct. 1985.
- [7] G. Schiavon, R. Sorrentino, and P. Tognolatti, "Characterization of coupled finlines by generalized transverse resonance method," *Int. J. Numer. Modelling.* vol. 1, pp. 45-59, Mar. 1988.
- [8] S. W. Lee, W. R. Jones, and J. J. Campbell, "Convergence of numerical solutions of iris-type discontinuity problems," *IEEE Trans. Microwave Theory Tech.*, vol. MTT-19, pp. 528-536, June 1971.
- [9] R. Mittra, T. Itoh, and T.-S. Li, "Analytical and numerical studies of the relative convergence phenomenon arising in the solution of an integral equation by the moment method," *IEEE Trans. Microwave Theory Tech.*, vol. MTT-20, pp. 96-104, Feb. 1972.
- [10] A. S. Omar and K. Schuenemann, "Space-domain decoupling of LSE and LSM fields in generalized planar guiding structures," *IEEE Trans. Microwave Theory Tech.*, vol. MTT-32, pp. 1626-1632, 1984.
- [11] N. Marcuvitz, *Waveguide Handbook*. New York, McGraw-Hill, 1951.
- [12] K. Mehmet *et al.*, "Simple resonator method for measuring dispersion of microstrip," *Electron. Lett.*, vol. 8, no. 6, pp. 165-166, 1972.
- [13] F. Alessandri, U. Goebel, F. Melai, and R. Sorrentino, "Theoretical and experimental characterization of nonsymmetrically shielded coplanar waveguides for millimeter wave circuits," in *1989 IEEE MTT-S Int. Microwave Symp. Dig.* pp. 1219-1222.

✉



Ferdinando Alessandri was born in Rome, Italy, on June 26, 1959. He received the Laurea degree in electronic engineering (summa cum laude) from the University of Rome "La Sapienza," Rome, Italy, in 1986.

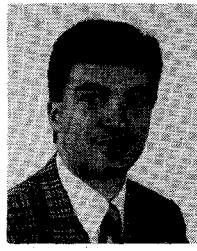
Since completing military service he has been with the University of Rome Tor Vergata and with industries such as Selenia Spazio S.p.a., Rome, and Micrel S.p.a., Florence, working on the modeling of passive microwave and millimeter-wave circuits.



Uhland Goebel was born in Bielefeld, West Germany, in 1954. He received the Dipl. Ing. degree in electrical engineering from the Technical University Braunschweig, West Germany, in 1983.

Since then, he has worked as a research assistant at the Technical University of Braunschweig (1983-1984) and the Technical University of Hamburg-Harburg, West Germany (1984-1988). He has done research on power-combined microwave oscillators, novel structures for nonreciprocal microwave devices and solid-state control, and mixer circuits for millimeter-wave applications. In 1989 he joined Micrel S.p.A. in Florence, Italy, where he is responsible for millimeter-wave component and subsystem development.

★



Franco Melai (M'88) was born in Empoli, Italy, on March 12, 1956. He received the "Laurea" degree (cum laude) in electronic engineering from the University of Pisa, Italy, in 1983.

He joined the Italian Navy in September 1983 as a technical officer. From March 1985 to July 1986 he was with Telettra S.p.A., Vimercate, Italy and from August 1986 to December 1987 he was with Marconi Italiana S.p.A., Genova, Italy, as a microwave engineer. Since January 1988 he is with Micrel S.p.A., Millimeter-Wave

Department, Firenze, Italy, where he is involved in the research and development of millimeter-wave components and subsystems.

Dr. Melai is a member of the Italian Electrical Society (AEI).

★



Roberto Sorrentino (M'77-SM'84) received the Laurea degree in electronic engineering from the University of Rome "La Sapienza," Rome, Italy, in 1971.

In 1971 he joined the Department of Electronics of the same university, where he was an Assistant Professor of Microwaves. He was also Professore Incaricato at the University of Catania (1975-1976), at the University of Ancona (1976-1977), and at the University of Roma "La Sapienza" (1977-1982), where he then was an Associate Professor from 1981 to 1986. In 1983 and 1986 he was a Research Fellow at the University of Texas at Austin. Since 1986 he has been Professor of Microwaves at the University of Rome "Tor Vergata." His research activities have been concerned with electromagnetic wave propagation in anisotropic media, interaction of electromagnetic fields with biological tissues, and mainly with the analysis and design of microwave and millimeter-wave integrated circuits.

Dr. Sorrentino is a member of the editorial boards of the IEEE TRANSACTIONS ON MICROWAVE THEORY AND TECHNIQUES, the International Journal on Numerical Modelling, and the Journal of Electromagnetic Waves and Applications (JEW).